

# Objective Evaluation of a Novel Filter-Based Motion Cueing Algorithm in Comparison to Optimization-Based Control in Interactive Driving Simulation

Patrick Biemelt, Sven Mertin, Nico Rüdtenklau, Sandra Gausemeier and Ansgar Trächtler

Chair of Control Engineering and Mechatronics, Heinz Nixdorf Institute, University of Paderborn, Germany

Email: {patrick.biemelt, sven.mertin, nico.rueddenklau, sandra.gausemeier, ansгар.traechtler}@hni.uni-paderborn.de

**Abstract**—Dynamic driving simulators have become a key technology to support the development and optimization process of modern vehicle systems both in academic research and in the automotive industry. However, the validity of the results obtained in simulator tests depends significantly on the adequate reproduction of the simulated vehicle movements and the associated immersion of the driver. Therefore, specific motion platform control strategies, so-called *Motion Cueing Algorithms* (MCA), are used to replicate the acting accelerations and angular velocities within the physical limitations of the driving simulator best possible. In this paper, we present a novel filter-based control approach for this task, using a hybrid kinematics motion system as an application example. Based on introduced quality criteria, an objective comparison of the proposed control strategy and a real-time capable *Model Predictive Control* (MPC) algorithm is performed using various standard driving scenarios. These include longitudinal as well as lateral dynamic maneuvers in order to estimate the overall improvements of both Motion Cueing Algorithms for interactive driving simulation.

**Keywords**—Driving Simulation; Human-in-the-Loop; Motion Cueing; Dynamic Motion Platform Control; Objective Quality Criteria.

## I. INTRODUCTION

Driven by topics, such as e-mobility and autonomous driving, in recent years there has been a continuous trend towards interconnectivity and multifunctionality of vehicle components, as well as Advanced Driver Assistance Systems (ADAS). As a consequence, automobile manufacturers and developers have to deal with increased product complexities and simultaneously decreased development periods to ensure their competitiveness in the automotive industry. To overcome those new technological challenges, the use of interactive driving simulators represents an indispensable tool to transfer the conventional development process, based on physical prototypes and on-road tests, to model-based test procedures. Such virtual prototyping methods using driving simulators provide the benefit of time and cost savings, as well as safe and reproducible test environments with a high level of flexibility at the same time. For example, varying weather and lighting conditions can be directly adapted to the test requirements in the simulated environment, which supports i.a. the development and optimization of modern headlamp systems significantly [1]. Furthermore, interactive driving simulation enables to access human-centered aspects, such as demonstration and marketing, driver training and behavior studies [2][3].

Disregarding from the particular analysis purpose, the validity of the results obtained in a virtual test drive is closely linked to the degree of immersion. Interactive driving simulation can therefore be characterized as a *Human- and Hardware-in-the-Loop* (HHIL) application whose transferability to real driving situations can only be guaranteed if a realistic driving impression is created. Hence, it is necessary to

provide the human perception system with all required motion information, so-called *Motion Cues*. In addition to the acoustic and visual stimuli, also the vestibular Motion Cues, more precisely the acting translational accelerations and angular velocities of the simulated vehicle, must be generated using the motion system of the dynamic driving simulator. For this reason, specific Motion Cueing Algorithms are applied in order to create a driving experience that is as realistic as possible within the physical limitations of the motion system.

The most common approach for this task is the *Classical Washout Algorithm*, which was first described by Schmidt and Conrad as a motion platform control algorithm for piloted flight simulators [4]. As illustrated in Figure 1, this MCA basically consists of a sequence of frequency divisions in order to generate suitable position and orientation reference signals for the simulator motion system. The high-frequency components of the scaled translational accelerations and angular velocities of the vehicle dynamics model are therefore separated using appropriate high-pass filters. Afterwards, these extracted components are directly integrated to a corresponding position and orientation of the driving simulator. Since the basic idea of this algorithm is to return the motion system to its neutral position after it has performed the high-frequency movements, a further high-pass filtering of the integrated signals is conducted. This is known as the *washout effect*, according to which the algorithm is named. Due to the typically small workspace, an analog integration of the low-frequency accelerations and angular velocities would lead the motion system very fast to its physical limits and thus cannot be performed. Hence, sustained accelerations are simulated via the *tilt coordination* technique, which makes use of the gravitational force to replicate these accelerations by an equivalent rotation of the driving simulator. The corresponding rotation rate is usually limited to the perception threshold of the human vestibular system in this process, so that the rotational motion will not be realized by the driver inside the simulator.

This simple control strategy has been extensively studied and improved since its first publication, typically using

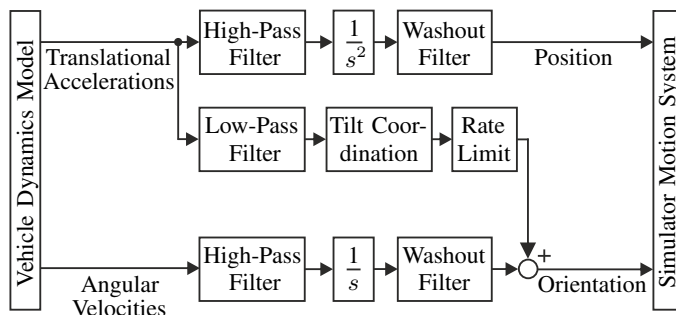


Figure 1. Scheme of the Classical Washout Algorithm [4].

hexapod-based motion systems [5][6]. As a result of this research, the filter-based MCA evolved into the standard approach in interactive driving simulation that offers major benefits in terms of transparency and traceability. Each parameter in the Classical Washout Algorithm has a clear physical meaning and a unique association to a single degree of freedom, which simplifies the tuning significantly. However, this basic idea of treating the translational accelerations and angular velocities independently results in the fact that this approach cannot be applied to every type of motion system. Otherwise, conflicting vestibular stimuli are generated under certain circumstances, e.g., if there exist interdependencies between translational and rotational degrees of freedom of the motion system like it is introduced in the next section with the ATMOS driving simulator.

In the present work, we propose a novel filter-based Motion Cueing Algorithm that enables a dynamic position washout to any point within the simulator workspace without considerably affecting the high-frequency motion rendering. This key feature is motivated by the considered motion system, but can also be applied to other systems, which offers general advantages for interactive driving simulation. The resulting control quality is evaluated by means of defined objective quality criteria, which take into account both measured and perceived quantities, including models of the human perceptual system. Based on this valuation metric, the developed filter-based MCA is compared online to a Model Predictive Control approach using established driving scenarios from the automotive industry, as well as everyday driving maneuvers.

The rest of this paper is structured as follows: Section II briefly describes the considered motion system and its specific features that have to be taken into account to ensure a realistic driving impression. In Section III, the developed filter-based control strategy is presented in detail. Subsequently, the objective valuation metric and the examined driving scenarios are introduced in Section IV. Sections V and VI finally discuss the obtained results and give concluding remarks.

## II. ATMOS DYNAMIC DRIVING SIMULATOR

Figure 2 shows the Atlas Motion System (ATMOS) driving simulator that is operated at the Heinz Nixdorf Institute in Paderborn as a reconfigurable development platform for primarily lighting-based ADAS. As illustrated, this simulator is equipped with a real vehicle chassis including all its control actuators, a seamless circular projection with 270 degree viewing angle, a 5.1 multichannel audio system, as well as a unique five-degree-of-freedom motion system to guarantee full immersion of the driver in the virtual environment. Moreover, the acting accelerations and angular velocities are recorded using an Inertial Measurement Unit (IMU) that is installed close to the driver's head position in order to rate the quality of the applied Motion Cueing strategy.

Different from conventional hexapods [7], the motion system of the ATMOS driving simulator is designed as a hybrid kinematics system, which is composed of two mechanically coupled components that can be actuated independently. To illustrate the functionality, Figure 3 shows an exploded view based on the multibody model of the system. The shaker system below the vehicle chassis is equipped with three crankshaft drives to perform vertical translational movements, as well as to rotate the driver around the roll and pitch axis. Thus, the shaker replicates the simulated vehicle movements



Figure 2. ATMOS Dynamic Driving Simulator.

relative to the road surface with exception of yaw movements and can further be used to increase the effect of the tilt coordination by expanding the rotational workspace of the motion system. In addition to the shaker, the motion platform performs movements along curved axes in lateral and longitudinal direction via actuated cross-undercarriages that are driven on V-shaped tracks. Because of these tilted tracks, each translational movement of the motion platform leads simultaneously to an additional rotation around the corresponding axes and a vertical displacement of the platform center point. As a direct consequence of these coupled kinematics, performing pure translational movements of the motion platform is not possible. This has to be considered in the design of the control algorithm in order to avoid conflicting sensory information, so-

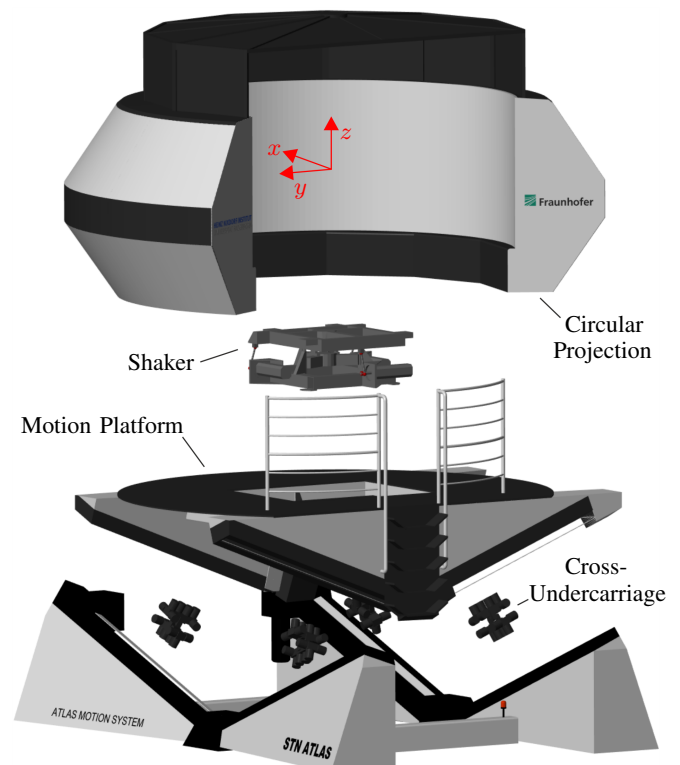


Figure 3. Exploded View of the Simulator Multibody Model.

called *False Cues*, which typically lead to the undesired effect of *Simulator Sickness* for the driver [8].

Due to the mentioned features of the ATMOS driving simulator, an extension of the conventional filter-based MCA is required since the implementation of the Classical Washout Algorithm according to Figure 1 does not result in the desired quality of the interactive driving simulation.

### III. DEVELOPED WASHOUT ALGORITHM

As described in Section I, the general idea of the Classical Washout Algorithm is based on an independent consideration of the systems degrees of freedom, which is due to the fact that the MCA was developed for application on a conventional hexapod. Because of this, the algorithm cannot be transferred to the ATMOS driving simulator introduced in the previous section, as there is a connection between translation and rotation because of the underlying kinematics of the motion system. For this reason, we subsequently present an extension of the classical approach that includes the relevant kinematic effects and enables a sufficient control quality.

#### A. Dynamic Position Washout

In case of the regarded driving simulator, each longitudinal and lateral movement of the motion platform generates a forced tilting around the corresponding roll and pitch axis. These rotations should ideally be used to emulate sustained accelerations using the tilt coordination technique. Otherwise, the tilt coordination has to be performed only by the shaker, which limits the maximum possible inclination to the small shaker workspace. In contrast to the classical algorithm, a dynamic position washout is therefore required that enables the motion platform to drift into a defined end position within its workspace after it has performed the high-frequency movements. By determining this end position according to the associated inclination, low-frequency accelerations can also be simulated via the motion platform. For this purpose, the high-pass (*hp*) and washout (*wo*) filters of the high-frequency longitudinal and lateral acceleration paths are supplemented by further first order low-pass filters with variable gains  $K$ , as shown in Figure 4 using the example of longitudinal acceleration  $a_x$ . The non-intuitive idea of this extension can be clarified by the application of the final value theorem of the Laplace transform. Therefore, let  $a_x$  be a sustained acceleration input from the vehicle dynamics simulation, which can be assumed to be approximately constant, since the magnitude does not significantly change. For the integrated simulator position  $x$  applies then with increasing time  $t$ :

$$\begin{aligned} \lim_{t \rightarrow \infty} x(t) &= \lim_{s \rightarrow 0} s \cdot X(s) \\ &= \lim_{s \rightarrow 0} s \cdot \frac{T_{hp}s + K}{T_{hp}s + 1} \cdot \frac{1}{s^2} \cdot \frac{T_{wo}^2 s^2}{T_{wo}^2 s^2 + 2DT_{wo}s + 1} \cdot \frac{a_x}{s} \\ &= K \cdot T_{wo}^2 \cdot a_x \end{aligned} \quad (1)$$

This yields a resulting simulator position  $x$  that depends on the gain  $K$ , the time constant  $T_{wo}$  of the washout filter as well as the amplitude of the acting acceleration  $a_x$ . If this position is now required to have a defined value  $x_{tc}$ , the necessary gain  $K$  can be determined corresponding to (1) as

$$K = \frac{x_{tc}}{T_{wo}^2 \cdot a_x}. \quad (2)$$

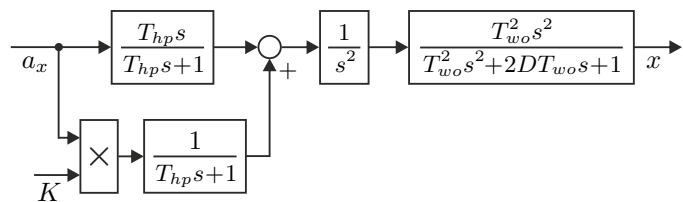


Figure 4. Extended Longitudinal High-Frequency Acceleration Path.

Analogously, the initial value theorem of the Laplace transform can be used to show that the extension by the variable gain low-pass filter, as shown in Figure 4, does not negatively affect the reproduction of high-frequency acceleration components. Like in the Classical Washout Algorithm, the dynamics of the drift into the end position  $x_{tc}$  can be influenced by the parameters of the washout filter, which is an additional design freedom in the parameterization of the developed algorithm.

The described extension is also implemented for the lateral high-frequency acceleration path, so that a washout in the defined position  $y_{tc}$  according to (2) is realized and thus sustained lateral stimuli are produced by a corresponding roll rotation of the motion platform.

#### B. Tilt Coordination Distribution

Due to the hybrid kinematics motion system, as well as the presented dynamic position washout, the tilt coordination technique can be performed either using the motion platform (*mp*), the shaker (*sh*) or a combination of both systems. The latter significantly increases the workspace and thus the maximum low-frequency acceleration amplitudes that can be generated. Consequently, a distribution strategy has to be specified, which enables a suitable coordination of both components. For this reason, an adaptation of the low-frequency longitudinal and lateral acceleration paths is conducted according to Figure 5. As shown with the example of the longitudinal acceleration, a first order low-pass filter (*lp*) extracts the sustained acceleration components from the reference signal  $a_x$ , which are subsequently converted to the corresponding tilt coordination pitch angle  $\theta_{tc}$ . In doing so, the associated rotation rate is limited to the well-established value of  $0.1 \text{ rad/s}$ , in order that the tilt coordination is not detected by the human driver [9]. In contrast to conventional hexapods, this inclination is divided among the subsystems of the motion system by introducing a distribution coefficient  $\alpha \in \mathbb{R}$  with  $0 \leq \alpha \leq 1$ . This results in the inclinations for the shaker  $\theta_{sh}$  and for the motion platform  $\theta_{mp}$  that are necessary to replicate the low-frequency accelerations by the gravitational force. Based on the kinematic relations of the motion platform, an equivalent platform position  $x_{tc}$ , which corresponds to the required inclination, is

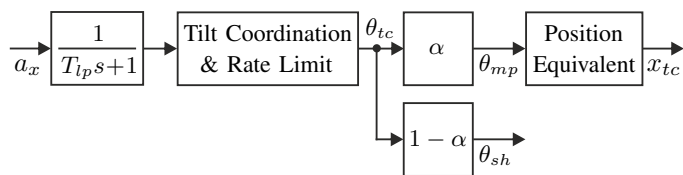


Figure 5. Extended Longitudinal Low-Frequency Acceleration Path.

subsequently determined. This position equivalent then serves as input for calculating the variable gain  $K$  according to (2) so that the coupling between translational and rotational degrees of freedom is taken into account. Equally, this process is implemented for the lateral low-frequency acceleration path.

### C. Resulting Algorithm Structure and Parameterization

The combination of dynamic position washout and tilt coordination distribution leads to the overall structure of the developed washout algorithm illustrated in Figure 6. Based on the idea of the Classical Washout Algorithm, this filter-based control strategy enables the generation of suitable control signals in the form of position and orientation commands for the motion system of the ATMOS driving simulator. The necessary estimation of the corresponding filter parameters and distribution coefficients was performed by numerical optimization using a defined driving maneuver. Here, the rural road drive, which will be introduced in the next section, was chosen since it represents a good compromise between moderate driving situations and extreme maneuvers at the limits of driving dynamics. Table I provides an overview of the resulting parameters.

Although the developed algorithm is motivated by the specific features of the motion system, in particular the concept of a dynamic position washout offers great potential for application in alternative control approaches. Thus, an integration in the context of lane-based algorithms is feasible, which use vehicle position information on the road to laterally reposition the motion system and therefore use the available workspace more effectively [6][10].

TABLE I. APPLIED ALGORITHM PARAMETERS.

Scaling	1st Order HP Filter	1st Order LP Filter	2nd Order WO Filter	Distribution Coefficient
$k_x = 0.4$	$T_{hp} = 0.95$	$T_{lp} = 0.95$	$T_{wo} = 0.49,$ $D = 0.7$	$\alpha_x = 0.65$
$k_y = 0.4$	$T_{hp} = 0.6$	$T_{lp} = 0.6$	$T_{wo} = 0.44,$ $D = 1.0$	$\alpha_y = 0.6$
$k_z = 1.0$	$T_{hp} = 0.4$	-	$T_{wo} = 0.45,$ $D = 1.0$	-
Scaling	1st Order HP Filter	1st Order LP Filter	1st Order WO Filter	Distribution Coefficient
$k_\varphi = 1.0$	$T_{hp} = 1.2$	-	$T_{wo} = 0.8$	-
$k_\theta = 1.0$	$T_{hp} = 0.3$	-	$T_{wo} = 0.2$	-

## IV. COMPARISON OF THE CONTROL STRATEGIES

The scientific objective in this contribution deals with the comparison of the filter-based MCA presented in Section III with an optimization-based approach using the concept of Model Predictive Control. This real-time capable predictive controller results from previous research and is described in detail in [11]. For that reason, only the basic idea of the algorithm is briefly discussed in this section. In addition, the applied quality criteria as well as the examined driving scenarios are introduced afterwards.

### A. Model Predictive Control Approach

According to the general concept of the MPC paradigm, an optimal control problem is numerically solved over a receding time horizon at each calculation cycle. Subsequently, only the first element of the computed control variable is applied to the process and the procedure is iterated. The application of this technique in terms of a Motion Cueing Algorithm leads to the structure shown in Figure 7. Based on the current system state  $x \in \mathbb{R}^{15}$ , which contains the angles, the angular velocities and the angular accelerations of all five actuators, the output vector  $y = [a^T \ \omega^T]^T \in \mathbb{R}^5$  is estimated within the prediction horizon  $N$ , depending on the reference angles of each actuator  $u \in \mathbb{R}^5$ . The MPC determines suitable system inputs so that the predicted outputs best possible match the vector of the reference accelerations and angular velocities  $r \in \mathbb{R}^{5N}$  from the vehicle dynamics simulation. In this approach, the accuracy of the control algorithm depends significantly on the availability of an adequate process model to predict the future system behavior. In case of the presented controller, the prediction model includes a linear model of the actuator dynamics, as well as the nonlinear kinematic relations of the motion system. This ensures that the relevant characteristics of the considered motion system described in Section II and its effects on the driver in the simulator are taken into account in the optimization process. At the same time, it is guaranteed that the determined actuating variables can be realized by the motion system, since its physical limits are included as constraints in the optimization problem. In that context, a first order approximation of the nonlinear system behavior at runtime presents a key feature of the developed predictive controller to meet the real-time requirements, which is the primary challenge in optimization-based MCA.

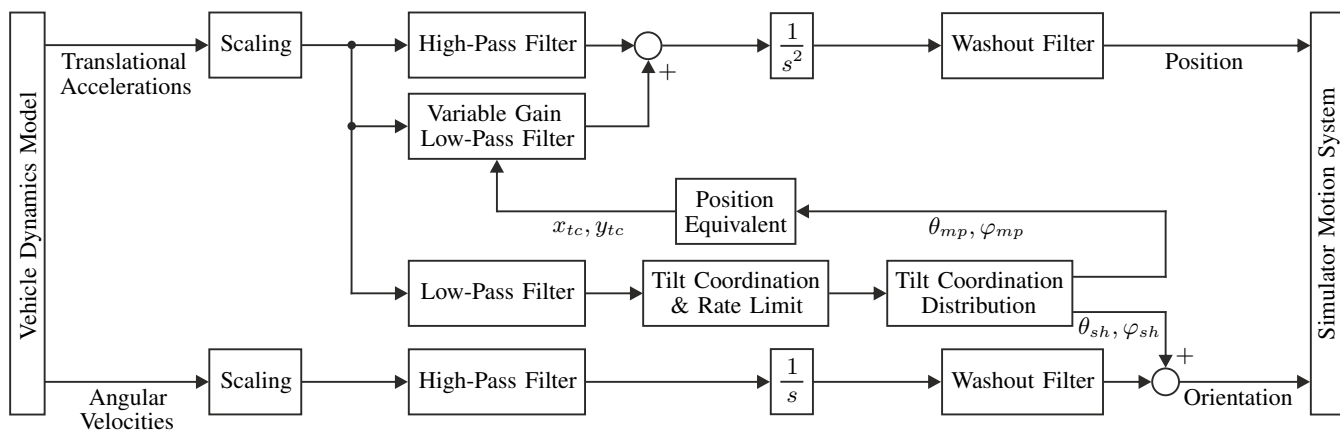


Figure 6. Overall Structure of the Developed Washout Algorithm.

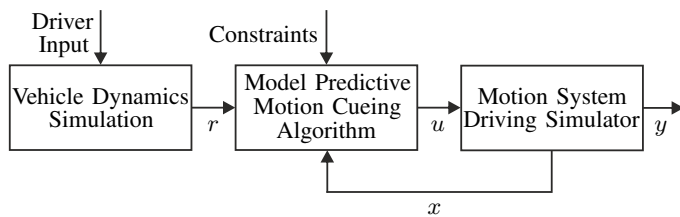


Figure 7. Scheme of the MPC-Based Control Algorithm.

### B. Objective Quality Criteria

In order to compare both Motion Cueing strategies on the basis of an objective valuation metric, suitable quality criteria must be specified. Therefore, according to [12] and [13], we introduce performance indicators  $\lambda_1$  and  $\lambda_2$  that are defined as

$$\lambda_1 = \frac{1}{N} \sum_{j=0}^N \sqrt{\left(\frac{e_{a_x,j}}{a_{x,norm}}\right)^2 + \left(\frac{e_{a_y,j}}{a_{y,norm}}\right)^2 + \left(\frac{e_{a_z,j}}{a_{z,norm}}\right)^2} + \frac{1}{N} \sum_{j=0}^N \sqrt{\left(\frac{e_{\omega_x,j}}{\omega_{x,norm}}\right)^2 + \left(\frac{e_{\omega_y,j}}{\omega_{y,norm}}\right)^2} \quad (3)$$

and

$$\lambda_2 = \frac{1}{N} \sum_{j=0}^N \sqrt{\left(\frac{e_{\hat{a}_x,j}}{a_{x,norm}}\right)^2 + \left(\frac{e_{\hat{a}_y,j}}{a_{y,norm}}\right)^2 + \left(\frac{e_{\hat{a}_z,j}}{a_{z,norm}}\right)^2} + \frac{1}{N} \sum_{j=0}^N \sqrt{\left(\frac{e_{\hat{\omega}_x,j}}{\omega_{x,norm}}\right)^2 + \left(\frac{e_{\hat{\omega}_y,j}}{\omega_{y,norm}}\right)^2} \quad (4)$$

with

$$\begin{aligned} e_{a_i} &= a_{i,Ref} - a_i|_{i=x,y,z} \quad \text{and} \quad e_{\omega_i} = \omega_{i,Ref} - \omega_i|_{i=x,y} \\ e_{\hat{a}_i} &= \hat{a}_{i,Ref} - \hat{a}_i|_{i=x,y,z} \quad \text{and} \quad e_{\hat{\omega}_i} = \hat{\omega}_{i,Ref} - \hat{\omega}_i|_{i=x,y}. \end{aligned} \quad (5)$$

Here, (3) provides a measure of the physical deviations between the scaled reference accelerations  $a_{i,Ref}$  and angular velocities  $\omega_{i,Ref}$  from the vehicle dynamics simulation and the measured quantities in the driving simulator for the considered degrees of freedom.  $\lambda_1$  therefore returns the averaged normalized control error over the number of measured values  $N$ . The normalization is necessary to obtain dimensionless quantities that allow a simultaneous consideration of accelerations and angular velocities in a common scale. According to [14], the human perception thresholds for movements are used as corresponding normalization factors  $a_{i,norm}$  and  $\omega_{i,norm}$ . In addition, the indicator  $\lambda_2$  according to (4) yields a measure for the perceived control quality, which can differ from the physical deviations due to the frequency-dependent dynamic behavior of the human vestibular organs, as well as perception thresholds. This causes, for example, that control errors in detectable frequency ranges are perceived more disturbing than deviations in undetectable ranges. To take these effects into account, well-established models of the vestibular system, more precisely the otoliths and semicircular canals, are included as they are shown in Figure 8. These usually contain mechanical analogous models of the respective organs, which lead to the illustrated transfer functions with the inputs  $a_i$  and  $\omega_i$  [15][16], as they are widely used in driving simulation applications [9].

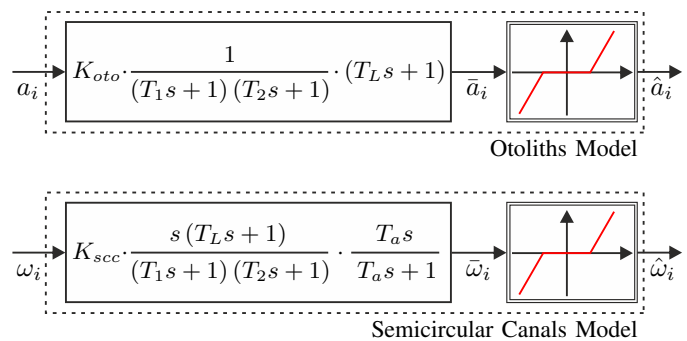


Figure 8. Applied Models of the Human Vestibular System.

By a series connection of the transfer functions with nonlinear dead zones, the threshold values  $a_{i,thres}$  and  $\omega_{i,thres}$  of the human perception are integrated with respect to the following relationship [5]:

$$\begin{aligned} \hat{a}_i &= \begin{cases} 0 & \text{if } |\bar{a}_i| \leq a_{i,thres} \\ \bar{a}_i - \text{sgn}(\bar{a}_i) \cdot a_{i,thres} & \text{if } |\bar{a}_i| > a_{i,thres} \end{cases} \\ \hat{\omega}_i &= \begin{cases} 0 & \text{if } |\bar{\omega}_i| \leq \omega_{i,thres} \\ \bar{\omega}_i - \text{sgn}(\bar{\omega}_i) \cdot \omega_{i,thres} & \text{if } |\bar{\omega}_i| > \omega_{i,thres} \end{cases} \end{aligned} \quad (6)$$

Consequently, the closer the performance indicators  $\lambda_1$  and  $\lambda_2$  are to the origin, the better is the reproduction of the simulated vehicle movements, whereby the value zero indicates a perfect motion rendering. However, especially with regard to  $\lambda_1$ , this is only a theoretical value that cannot be obtained by any driving simulator, since it would require an almost unlimited workspace.

### C. Driving Scenarios

For the purpose of obtaining a representative comparison of the two control strategies, a selection of nine driving scenarios was defined. These contain standardized maneuvers, which are commonly used for development and optimization applications in the automotive industry, like:

- Acceleration from standstill
- Braking from driving straight forward (DIN ISO 70028)
- Lane change (DIN ISO 3888-1)
- Step steering (DIN ISO 7401)
- Braking from steady-state circular course drive (DIN ISO 7975)

As the listed maneuvers are mainly used to identify and analyze the driving dynamics of a vehicle, they do not represent usual driving situations. For this reason, also moderate scenarios are examined in the evaluation:

- Turning at a junction
- Drive on a rural road
- Drive through a roundabout
- Drive through a highway interchange

Vehicle dynamics simulations of all nine maneuvers were performed and the relevant accelerations and angular velocities were recorded. Subsequently, these data were used as identical reference signals for both MCA to ensure a consistent basis for evaluation described in the next section.

V. RESULTS AND DISCUSSION

Subsequently, the results of the comparison of the two Motion Cueing strategies are presented and the impacts on the interactive driving simulation are discussed. For that purpose, both control algorithms were implemented on the ATMOS driving simulator. Measurement data of the translational accelerations and the angular velocities taken with the installed IMU at the driver’s head position serve as inputs for the quality criteria presented in Section IV. For reasons of clarity, only measured data of the maneuver “turning at a junction” are analyzed in detail (see Figures 9, 10, 11). All further driving scenarios are summarized in Figure 12.

Figure 9 shows the resulting longitudinal acceleration and pitch velocity tracking. It becomes clear that both the proposed washout algorithm and the optimization-based approach yield an adequate reproduction of the longitudinal acceleration from the vehicle dynamics simulation. However, the measured accelerations show a larger time delay in comparison to the reference signal when using the washout algorithm due to the phase shift of the implemented filters. The corresponding pitch velocity contains in both cases low-frequency disturbances that can be explained by the tilt coordination, since the sustained acceleration can only be reproduced by an equivalent rotation of the motion system. Using the washout algorithm, these errors are significantly higher, so it can be expected that the resulting driving experience will be negatively affected. In contrast, the predictive MCA uses the available model knowledge to limit the overall rotation rate error to the value of  $0.1 \text{ rad/s}$ . Equivalent results can be derived from Figure 10, which illustrates the lateral acceleration and the corresponding roll velocity. Also in this case, the acceleration reference from the vehicle dynamics simulation is tracked very well with both algorithms. There are again time delays to the reference signal that are larger when using the washout algorithm, due to the nature of the implemented filters. The roll velocity error is also

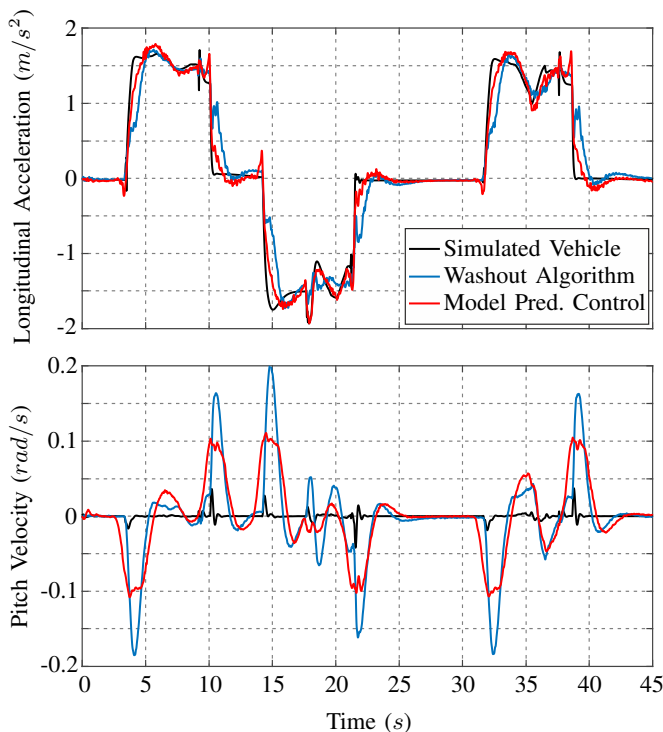


Figure 9. Longitudinal Acceleration and Pitch Velocity Tracking.

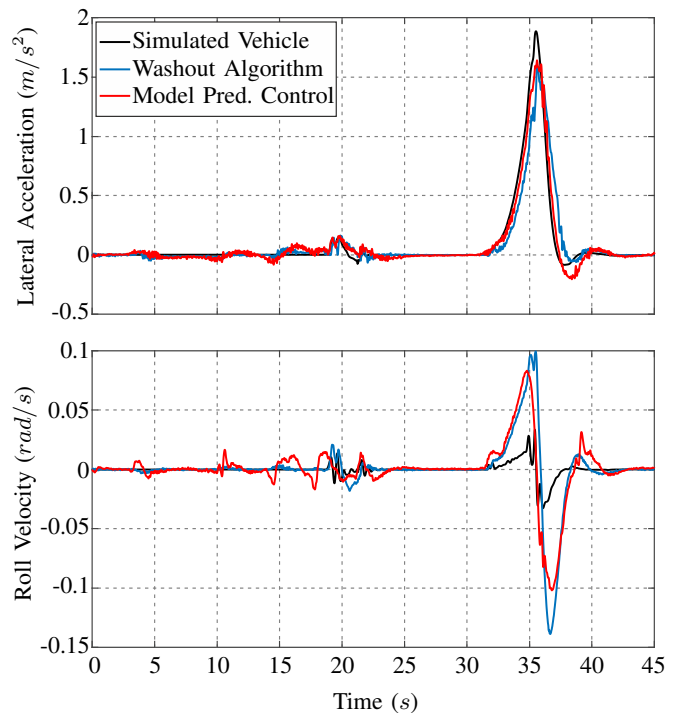


Figure 10. Lateral Acceleration and Roll Velocity Tracking.

larger than that of the MPC, even if the difference is smaller than in case of the pitch velocity. Thus, as a consequence for the interactive driving simulation, the resulting driving experience can be expected to be more realistic using the predictive control strategy, since smaller rotation rate errors are more difficult to detect for the human perception system. The vertical acceleration measured in the regarded driving scenario is illustrated in Figure 11. Here, it is noticeable that undesired vertical displacements occur due to the coupled degrees of freedom of the motion system, which cannot be compensated by any of the two approaches. However, these unpreventable errors are significantly lower and mostly below the perception threshold of the otoliths in the use of the predictive MCA, which can be explained by a more efficient coordination of the shaker and the motion platform. Regarding the examined driving maneuver, the application of the quality criteria introduced in the previous section results in the performance indicators  $\lambda_{1,WO} = 1.74$  and  $\lambda_{2,WO} = 0.92$  for the washout algorithm and  $\lambda_{1,MPC} = 1.20$  and  $\lambda_{2,WO} = 0.53$  for the predictive controller. This confirms the impression that the MPC-based algorithm achieves a higher control quality, which is primarily explained by the lower angular velocity and

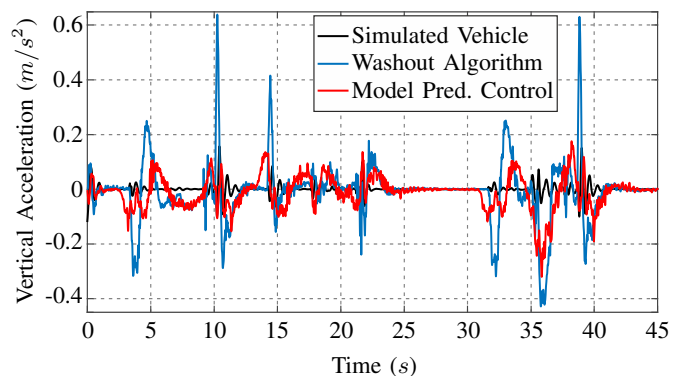


Figure 11. Vertical Acceleration Tracking.

vertical acceleration errors caused by the specific kinematics of the ATMOS driving simulator.

Figure 12 combines the evaluation of all nine test maneuvers in a common radar chart. The analysis of this graphic clearly shows the advantages of the optimization-based MCA in comparison to the washout algorithm, since smaller performance indicators are achieved in each scenario. It is noticeable that the perceived control quality, expressed by the indicator  $\lambda_2$ , yields small values close to zero when the MPC is used and therefore a good subjective driving impression can be expected. As already discussed in detail for driving maneuver “turning at a junction”, these results can be explained with the angular velocity and vertical acceleration errors due to the coupled degrees of freedom, because of which an adequate reproduction of the simulated vehicles Motion Cues is a challenging task. Here, it is a great advantage of the MPC that the specific simulator kinematics are directly considered via existing model knowledge in the optimization algorithm. This allows undesired interactions to be taken into account in the planning of the motion trajectory and optimally compensated according to the current driving situation, which is a major benefit for interactive driving simulation.

## VI. CONCLUSION AND FUTURE WORK

In this paper, the development of a novel filter-based Motion Cueing Algorithm was presented. Motivated by the regarded hybrid kinematics motion system, the proposed algorithm features a dynamic position washout to any point within the simulator workspace, as well as a tilt coordination distribution strategy in order to make full use of the motion capabilities. Furthermore, this MCA was compared to a MPC-based algorithm by means of defined quality criteria and standard driving scenarios from the automotive industry. The objective evaluation of both Motion Cueing strategies proved a satisfactory control quality. However, due to the integration of model knowledge, the predictive MCA exhibits less control errors in angular velocities and vertical acceleration. For this reason, it is assumed that the subjective driving impression is more realistic when using the MPC, which is why this approach offers great potential for interactive driving sim-

ulation. On the other hand, the filter-based MCA has the advantages of simple implementation, good traceability and low computational effort, which relativizes the worse control quality in comparison to the optimization-based algorithm.

The future work will deal with the subjective validation of our observations. In this context, appropriate subject studies will be conducted in order to rate the resulting degree of immersion by human drivers. Besides, current research concentrates on the prediction of the future driver behavior and the associated reference trajectory for the model predictive MCA. Since the human driving behavior is predictable within certain limitations, a virtual driver model is applied to estimate the driver inputs within the time-limited prediction horizon at runtime.

## REFERENCES

- [1] N. Rüdtenklau, P. Biemelt, S. Henning, S. Gausemeier, and A. Trächtler, “Real-Time Lighting of High-Definition Headlamps for Night Driving Simulation,” *International Journal On Advances in Systems and Measurements*, vol. 12, 2019, pp. 72–88.
- [2] V. Melcher, S. Rauh, F. Diederichs, H. Widroither, and W. Bauer, “Take-Over Requests for automated driving,” *Procedia Manufacturing*, vol. 3, 2015, pp. 2867–2873.
- [3] H. Bellem et al., “Can We Study Autonomous Driving Comfort in Moving-Base Driving Simulators? A Validation Study,” *Human Factors*, vol. 59, no. 3, 2017, pp. 442–456.
- [4] S. F. Schmidt and B. Conrad, “Motion Drive Signals for Piloted Flight Simulators,” I Contract Report NASA, CR-1601, 1970.
- [5] L. D. Reid and M. A. Nahon, “Flight Simulation Motion-Base Drive Algorithms: Part 1 - Developing and Testing the Equations,” University of Toronto, UTIAS Report 296, 1985.
- [6] T. Sammet, “Motion-Cueing-Algorithmen für die Fahrsimulation (Motion Cueing Algorithms for Driving Simulation),” *Fortschritt Berichte-VDI Reihe 12 Verkehrstechnik/Fahrzeugtechnik*, vol. 643, 2007.
- [7] D. Stewart, “A Platform with Six Degrees of Freedom,” *Proceedings of the Institution of Mechanical Engineers*, vol. 180, no. 1, 1965, pp. 371–386.
- [8] D. Ariel and R. Sivan, “False Cue Reduction in Moving Flight Simulators,” *IEEE Transactions on Systems, Man, and Cybernetics*, no. 4, 1984, pp. 665–671.
- [9] M. Bruschetta, F. Maran, and A. Beghi, “A fast implementation of MPC-based motion cueing algorithms for mid-size road vehicle motion simulators,” *Vehicle System Dynamics*, vol. 55, no. 6, 2017, pp. 802–826.
- [10] J. O. Pitz, “Vorausschauender Motion-Cueing-Algorithmus für den Stuttgarter Fahr Simulator (Predictive Motion Cueing Algorithm for the Stuttgart Driving Simulator),” PhD Thesis, Universität Stuttgart, 2017.
- [11] P. Biemelt, S. Henning, N. Rüdtenklau, S. Gausemeier, and A. Trächtler, “A Model Predictive Motion Cueing Strategy for a 5-Degree-of-Freedom Driving Simulator with Hybrid Kinematics,” *Driving Simulation Conference Europe 2018 VR (DSC)*, 2018, pp. 79–85.
- [12] N. A. Pouliot, C. M. Gosselin, and M. A. Nahon, “Motion Simulation Capabilities of Three-Degree-of-Freedom Flight Simulators,” *Journal of Aircraft*, vol. 35, no. 1, 1998, pp. 9–17.
- [13] I. Al Qaisi and A. Trächtler, “Human in the Loop: Optimal Control of Driving Simulators and New Motion Quality Criterion,” in *2012 IEEE International Conference on Systems, Man, and Cybernetics (SMC)*. IEEE, 2012, pp. 2235–2240.
- [14] P. Grant, M. Blommer, B. Artz, and J. Greenberg, “Analysing Classes of Motion Drive Algorithms Based on Paired Comparison Techniques,” *Vehicle System Dynamics*, vol. 47, no. 9, 2009, pp. 1075–1093.
- [15] L. R. Young and J. L. Meiry, “A Revised Dynamic Otolith Model,” *Aerospace Medicine*, vol. 39, no. 6, 1968, pp. 606–608.
- [16] C. Fernandez and J. M. Goldberg, “Physiology of Peripheral Neurons Innervating Semicircular Canals of the Squirrel Monkey. II. Response to Sinusoidal Stimulation and Dynamics of Peripheral Vestibular System,” *Journal of Neurophysiology*, vol. 34, no. 4, 1971, pp. 661–675.

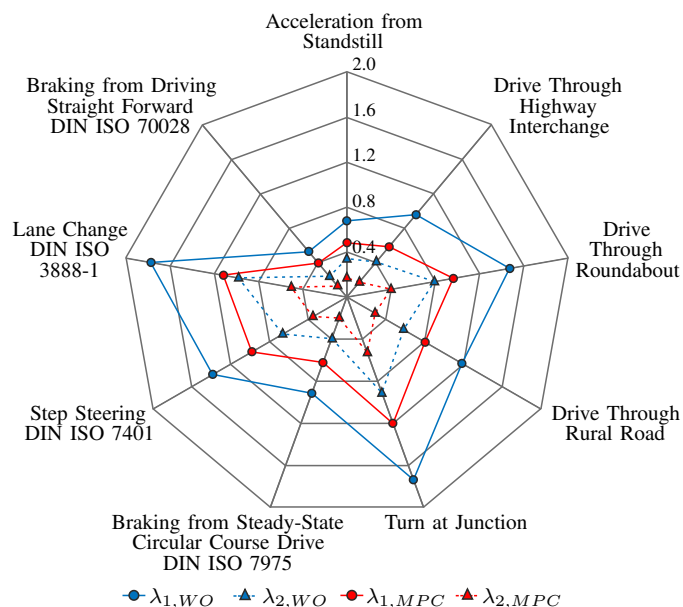


Figure 12. Evaluation of the Analyzed Test Maneuvers.